Preparation of Poly(vinylidene fluoride) Lithium-Ion Battery Separators and Their Compatibilization with Ionic Liquid - A Green Solvent Approach

Carlos M. Costa, *[a,b] Henrique M. Rodrigues, [a] Attila Gören, [a,b] Ana V. Machado, [c] Maria M. Silva, [b] and Senentxu Lanceros-Méndez* *[d,e]

Battery separator membranes for lithium-ion batteries have been developed based on poly(vinylidene fluoride), PVDF, and using the "green solvent" - N,N'-dimethylpropyleneurea (DMPU). This separator presents a porous microstructure with a degree of porosity of 20% and pore size below 1μ m, showing excellent mechanical properties. Further, its ionic conductivity, tortuosity and MacMullin number values are $0.1 mS.cm^{-1}$, 4 and 82, respectively. This PVDF separator membrane was evaluated in $Li/C-LiFePO_4$ half-cells with electrolyte solution showing good cyclability and rate capability, with a discharge value after 50 cycles of $56 mAh.g^{-1}$ at C, corresponding to 50% of the capacity retention. Its electrochemical performance soaked in ionic liquid presents a discharge capacity of $45 mAh.g^{-1}$ at C/5rate and capacity retention of 60%, respectively. Thus, this separator is an appropriate candidate for environmentally friendlier and safer lithium-ion batteries.

Introduction

High-power and high-energy density energy storage devices are essential for many applications such as mobile phones, watches, computers, e-labels and e-packaging, among others, and the constant development of new materials is mandatory to keep up with the fast technological development. [1]

Lithium-ion batteries are the type of energy storage systems more adequate for portable electronic devices being also intensively studied for the next generation of hybrid electric vehicles (PHEVs) and electric vehicles (EVs). [2]

Considering the environmental issues, this battery type is appropriate for storing the energy produced by renewable energy sources such as solar, wind or biomass. [3] The global market related to rechargeable battery of portable devices is dominated by lithium-ion batteries with approximately 75% share. This is due to their excellent characteristics, including high energy density (210Wh. kg^{-1}), high-operation voltage ($2.5 - 5.0$ V), low self-discharge rate ($2 - 8\%$ per month), flexible and lightweight design and longer lifespan (> 1000 cycles). [4] Specific energy, power, safety and reliability are nevertheless key issues that must be improved in lithium-ion batteries.

In this context, the separator membrane plays a relevant role, as it serves as a medium for lithium ion transfer between both electrodes (anode and cathode), control the number of lithium ions and their mobility and affects the overall battery performance. [5] The performance of battery separator membranes is determined by a large diversity of requirements, such as low ionic strength, mechanical and dimensional stability, resistance to thermal and chemical degradation by electrolyte impurities and chemical reagents, to be easily wetted by liquid electrolytes and to show uniform thickness. [5a,6] The functionality of the separator membrane is typically influenced by several parameters such as degree of porosity, average pore size- and tortuosity. [5a]

The most used polymers for the fabrication of separator membranes are poly(ethylene) (PE), [7] poly(propylene) (PP), [8] poly(ethylene oxide) (PEO), [9] poly(acrylonitrile) (PAN), [10] poly (methyl methacrylate) (PMMA), [11] and poly(vinylidene fluoride) (PVDF) [12] and its copolymers poly(vinylidene fluoride-co-trifluoroethylene) (P(VDF-TrFE)), [13] poly(vinylidene fluoride-co-hexafluoropropylene), (P(VDF-HFP)), [14] and poly(vinylidene fluoride-co-chlorotrifluoroethylene), (P(VDF-CTFE)). [15]

PVDF and its copolymers have been intensively investigated for battery separator membranes due to their high polarity, excellent thermal and mechanical properties, [16] controllable porosity and wettability by organic solvents, and chemical inertness and stability in cathodic environment. [5a] Separator membranes based on PVDF show high ionic conductivity mainly related to the high dielectric constant ($\varepsilon = 6 - 12$) of this polymer, which contributes to enhance ionic dissociation of the electrolyte. [17]

Typically, PVDF is dissolved in aprotic polar solvents such as N,N-dimethylformamide (DMF), dimethyl sulfoxide (DMSO), triethyl phosphate (TEP), N-methylpyrrolidone (NMP) or dimethylacetamide (DMAc) and porous membranes are obtained by thermally induced phase separation (TIPS) what is a suitable manufacturing method. [18] These solvents have several common characteristics such as being toxic, hazardous and dangerous to use at large scale. [19]

In this context, replacing the aforementioned solvents by environmentally friendlier ones, the so called "green" solvents, aiming to minimize environmental impact, improving solubilizing properties, biodegradability, safety and health issues is extremely relevant. [20]

It would be also important to use natural polymers as cellulose [21] and lignin [22] as battery separators, but at the present moment their performance is far from being adequate. Thereby and taking also into account the growth of the battery market, which increase the requirement of environmental issues, the goal of this work is to produce

porous PVDF membranes replacing the conventionally used dangerous solvent by the "green" solvent, N,N'-dimethylpropyleneurea (DMPU), which is characterized by high boiling and low melting temperatures, extremely low toxicity and for being considered a healthy solvent [23] for the first time in the literature. In order to increase the compatibility between $C - LiFePO_4$ cathodes and the new PVDF separator, the cathode films were produced with the same polymer type and solvent. The morphology, polymer phase, thermal, mechanical and electrical properties were determined. Then, the cycle performance and rate capabilities were evaluated using the conventional electrolyte solution and compared to glass microfiber separators. Finally, in order to obtain an environmentally friendlier lithium-ion battery, the conventional electrolyte was replaced by an ionic liquid, 1-ethyl-3-methylimidazolium bis(trifluoromethylsulfonyl) imide, $[C_2mim][NTf_2]$. [24]

Results

Morphology, polymer phase, thermal and mechanical properties

The morphology of the PVDF membrane crystallized at $50°C$ is presented in Figure 1. The morphology of the PVDF membranes depends on solvent evaporation temperature and polymer concentration, [25] therefore in the present case, the processing conditions were selected in order to obtain a porous microstructure with pores uniformly distributed along the surface and thickness of the membrane (Figure 1). The formation of the porous microstructure observed in Figure 1 is explained by the phase separation between polymer and solvent where the low crystallization temperature leading to a reduced polymer chains mobility, hindering the polymer to occupy the free space left by the evaporated solvent. [25]

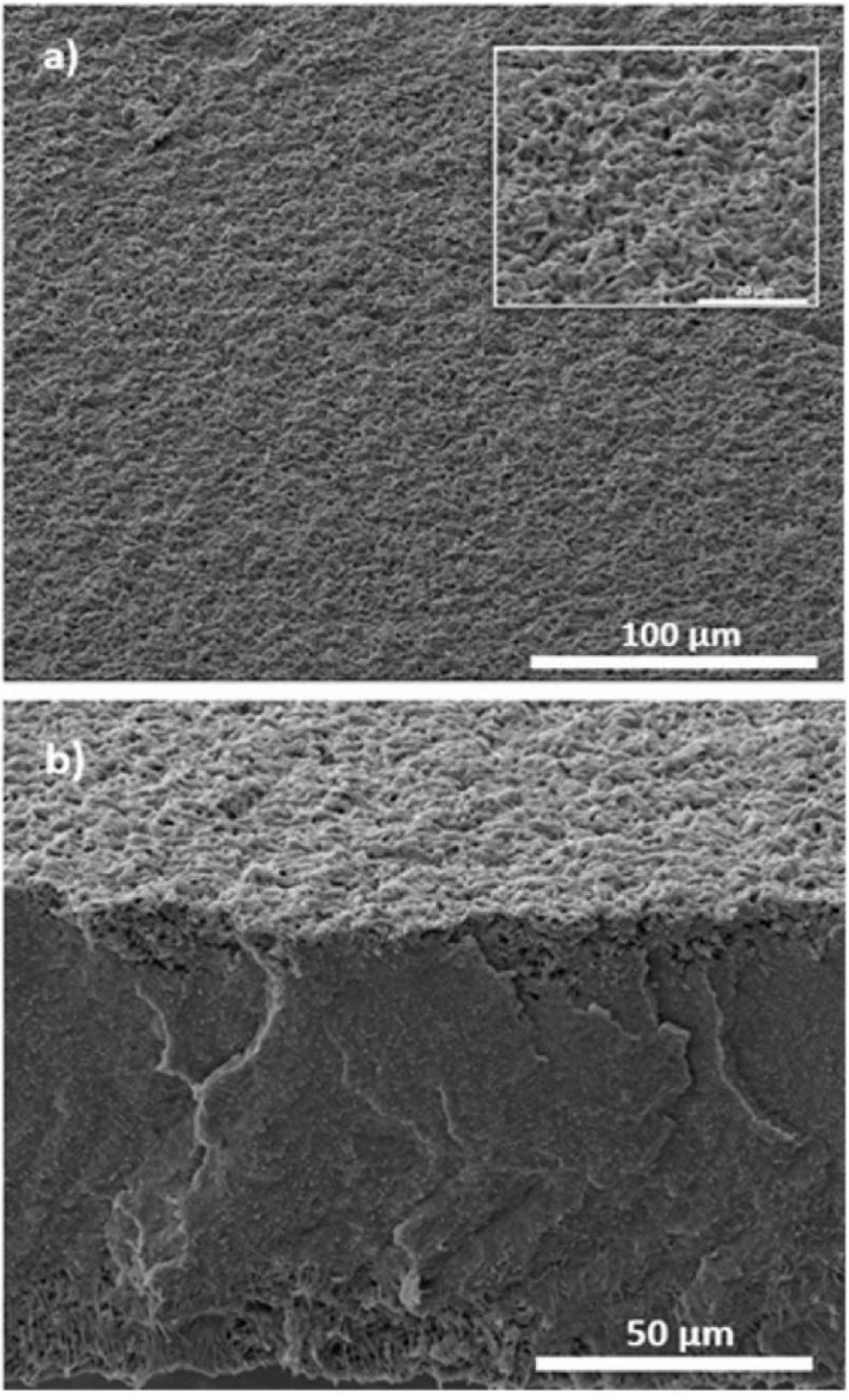
a)
100 µm
b)
50 µm

Figure 1. SEM micrographs of PVDF membrane in surface (a) and crosssection images.

The cross-section image (Figure 1b) shows an slightly inhomogeneous distribution of the pores along the thickness of the separator. This fact is due to the inhomogeneous solvent evaporation: the top surface is formed first on the interface between the environment and the polymer solution, whereas the bottom surface is in contact with glass plate.

The porous microstructure of the PVDF membrane is characterized by a low degree of porosity, small pore size (below 1μ m) and polymer crystallization in spherulites with a small radius of ~ 1μ m. The low degree of porosity, attributed to phase separation process between polymer, is ascribed to the low volatility of the DMPU solvent (low vapor pressure: 0.49 mmHg at 57°C). [26]

The degree of porosity, calculated by equation 2, is approximately 20%. It is to notice that the degree of porosity is lower than the typically used for commercial separators (~ 40%) for lithium ion batteries. [27] This degree of porosity is nevertheless interesting for the present application, as it allows to maintain the mechanical robustness of the membrane. Further-

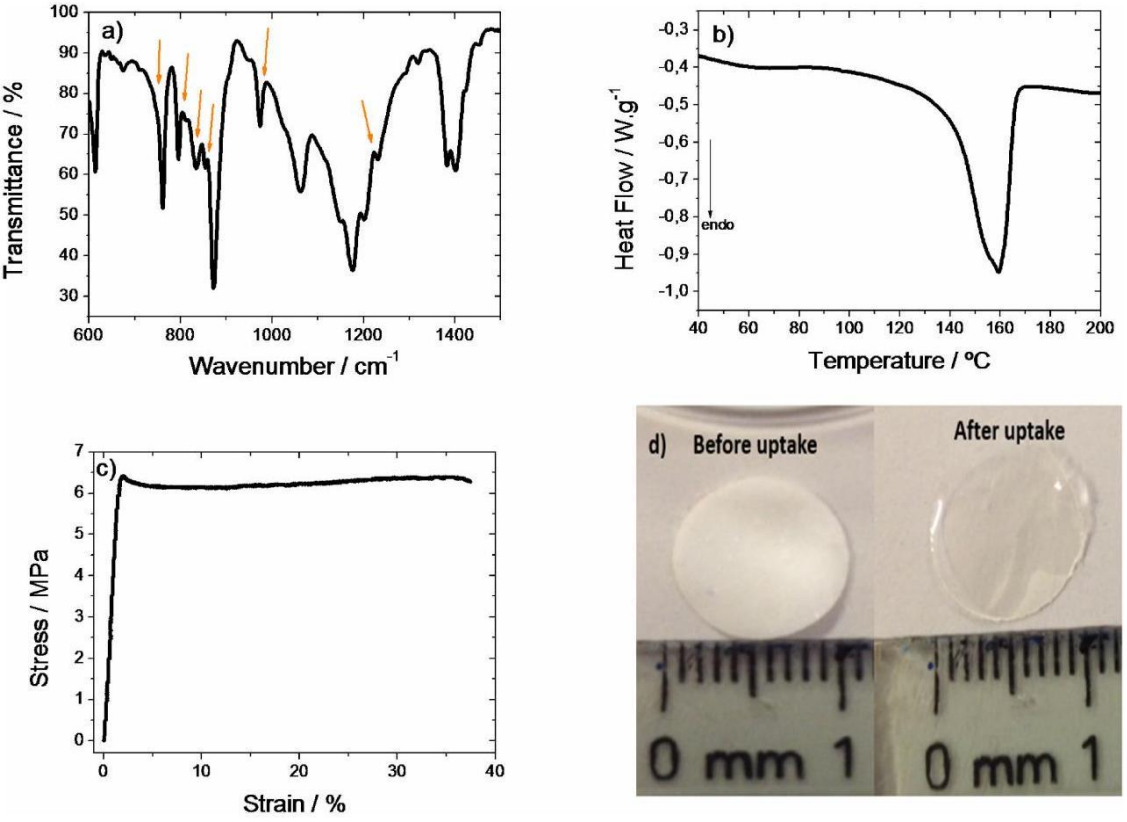

Figure 2. FTIR-ATR spectra (a), DSC scan (b), stress-strain curve (c) and swelling process (d) of the PVDF membrane.

more, a pore size below 1μ m inhibits dendritic lithium and prevents particles from penetrating inside the separator. [28]

Polymer crystalline phase, thermal and mechanical properties of the PVDF membrane were determined by FTIR, DSC and stress-strain measurements in the tensile mode, respectively (Figure 2).

The infrared spectrum of the PVDF membrane (Figure 2a) is characterized by the vibrational modes of the α-and β-phase of PVDF, which are identified by the arrows at 765, 796, 855 and 976 cm^{-1} for the α-phase and the ones at 840 and 1232 cm^{-1} for the β-phase. [16] The crystalline phase of PVDF is essentially affected by the solvent evaporation temperature and for low evaporation temperature up to 90°C, the crystallization is slow due to lower polymer-chain mobility and leads to preferential nucleation in β-phase. [16]

The DSC thermogram (Figure 2b) is characterized by a broad melting peak between 105°C to 171°C, with a maximum at 160°C. This peak represents the melting of the crystalline phase and its broad shape indicates a distribution of crystallite sizes. It can be also observed the thermal stability of the polymer up to 100°C, which is suitable for battery applications. The degree of crystallinity of the PVDF membrane is 52% (calculated by equation 1), which is typical for PVDF membranes. [25]

TGA curve (Figure S2, see supporting information) shows that the PVDF membrane just presents one degradation stage beginning at 390°C. Thus, the thermal stability of the PVDF membranes is similar to the one of PP separators (320°C).

For battery separators, the mechanical properties are one of the critical factors, as they affect integrity and safety of the battery. Figure 2c presents the stress-strain curves for the PVDF membrane, which shows the typical features obtained for thermoplastic, with two well defined regions indicative of the elastic and plastic deformation regimes.

Young modulus, the maximum of stress and strain of the PVDF membrane are 4.38MPa, 6.40MPa and 37%, respectively, which is appropriate for lithium-ion batteries.

Uptake and electrochemical properties

The swelling process is essential in battery separators, as it enhances the mobility of the polymer chains, and results in an increase of the polymer volume due to the interaction between the solvent molecules present in the electrolyte solution and the polymer chains. [29]

The swelling process of the PVDF membrane immersed in 1M$LiPF_6$ in EC/DEC is fast (Figure 3a) and mechanically stable, i.e, without fragmentation. After swelling, the sample remains transparent, which is originated by the gelatinization process (Figure 2d).

Figure 3a) shows the uptake of the electrolyte solution by the PVDF membrane as a function of the dipping time. It is shown that the process is very fast and 80% of the uptake takes place in 15 s , which is attributed to the strong interactions of the organic solvent present in the electrolyte solution and the polar functional groups from PVDF. [16]

The PVDF membrane achieves saturation after approximately 10 min with 98% of uptake value indicating that the void volume was fully filled with the electrolyte solution.

Impedance electrochemical spectroscopy was applied to determine the ionic conductivity at different temperatures (Figure 3b).

Figure 3b shows the Nyquist plot of the PVDF membrane at 25°C and 50°C and the ionic conductivity was calculated by

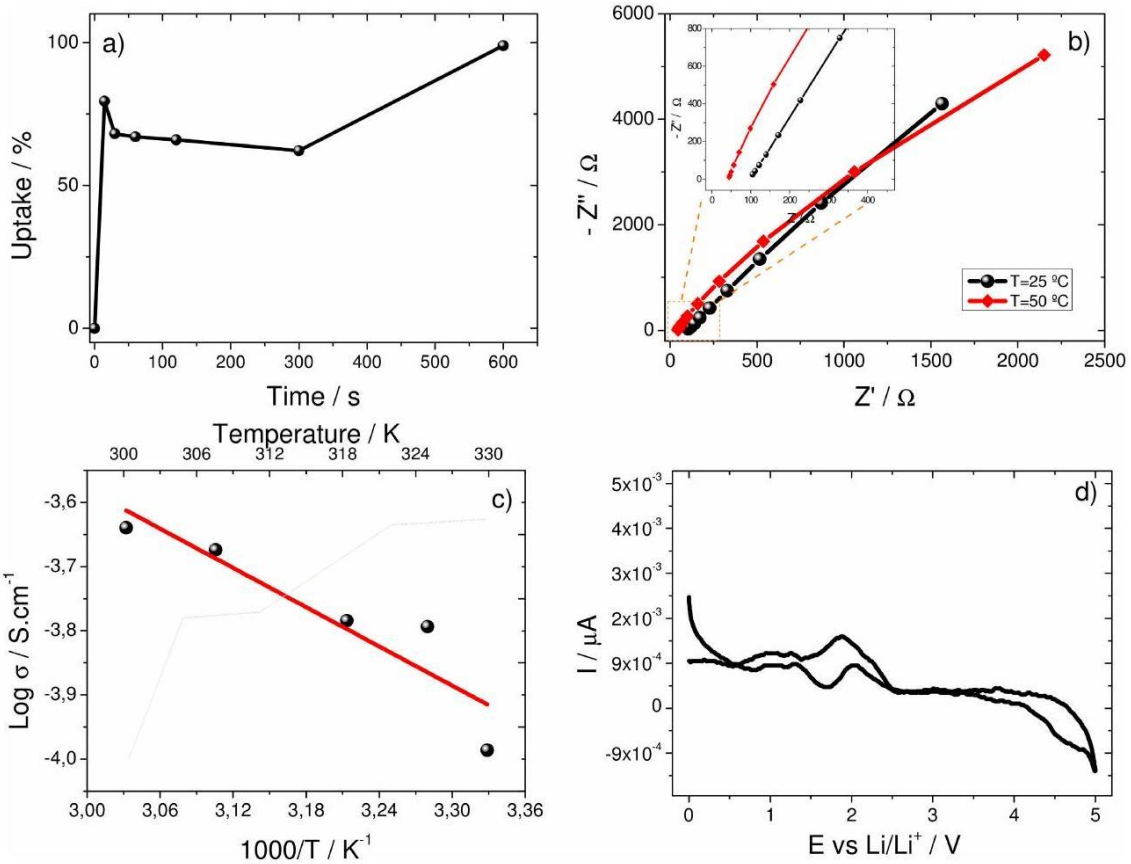

Figure 3. a) Uptake as a function of time, (b) Nyquist plots at 25°C and 50°C, (c) ionic conductivity as a function of the different temperatures and (d) electrochemical stability of the PVDF membrane.

equation 4 where the resistance of the bulk electrolyte was determined by the intercept of the imaginary impedance (minimum value of Z'') with the slanted line in the real impedance (Z').

The Nyquist plot is characterized by three different regions: a semicircle located at the high-frequency range, which is related to bulk resistance and to the geometric capacitance of the separator and electrolyte, a straight line at lower frequencies that is related to the diffusion process, and the transition between these phenomena. [30] In the Nyquist plots of Figure 3b and independently of the temperature, the total conductivity is due to ionic conduction. [31]

At room temperature ($T = 25°C$), the ionic conductivity, tortuosity and MacMullin number values, calculated after eq. 4, 6 and 7, are $0.1 mS.cm^{-1}$, 4 and 82, respectively. Taking into account that the ionic conductivity is above $10^{-4}\ S.cm^{-1}$, this PVDF

membrane can be applied as battery separator for lithium-ion batteries. Further, the low value of the tortuosity ($\tau = 4$) indicates high pore connectivity, leading to faster ion transport properties and, consequently, to high battery cycling performance and rate capability. [15] The MacMullin number that describes the influence of the porous microstructure of the separator, [32] it is observed that its value depends on the degree of porosity and electrolyte uptake value of the PVDF membrane correlated with ionic conductivity value. In the literature, its value are between ~ 6.5 to 18 for commercial separators. [32]

Figure 3c) shows the ionic conductivity as a function of temperature between $20°C$ and $70°C$. The results indicate that the ionic conductivity increases with increasing temperature due to the intrinsic property of the liquid electrolyte and to the increase of the free volume and segmental mobility of the polymer with increasing temperature. [15] This behavior is described by the Arrhenius model and the activation energy for ion transport is calculated by fitting equation 5 to the results shown in Figure 3c). The activation energy (Ea) is 8 ± 2 $kJ.mol^{-1}$, indicating a weak dependence of the conductivity on temperature, which is an advantage for battery applications.

The electrochemical window stability is a key parameter to evaluate battery performance and was evaluated by cyclic voltammetry in the potential range from 0.0 to 5.0 $V(vs.\ Li_{/Li^+})$ at the low scan rate of $5mV.s^{-1}$. The cyclic voltammogram of the PVDF membrane is shown in Figure 3d) showing a very small current flow until 5.0 V (vs. Li/Li^+) without significant electrochemical decomposition of the PVDF membrane and the electrolyte solution. Thus, it is shown that the PVDF membrane has a stability window until 5.0 V what is sufficient for practical applications in lithium ion batteries with certain cathodes such as $C - LiFePOO_4 \cdot$ [33]

Battery performance for 1 M LiPF6 in EC:DEC

In order to evaluate the battery performance of the PVDF membrane as battery separator in rechargeable lithium-ion batteries, $Li/C - LiFePO_4$ cathodic half-cells were fabricated and the results are shown in the Figure 4.

Charge-discharge curves at different C-rates from C/5 to 2C of the PVDF membrane in the fifth cycle are shown in Figure 4a).

The typical flat plateau of the C - $LiFePO_4$ cathodes reflects the reversible charge (lithium deinsertion)-discharge (lithium insertion) behavior. This behavior corresponds to the Fe^{2+}/Fe^{3+}

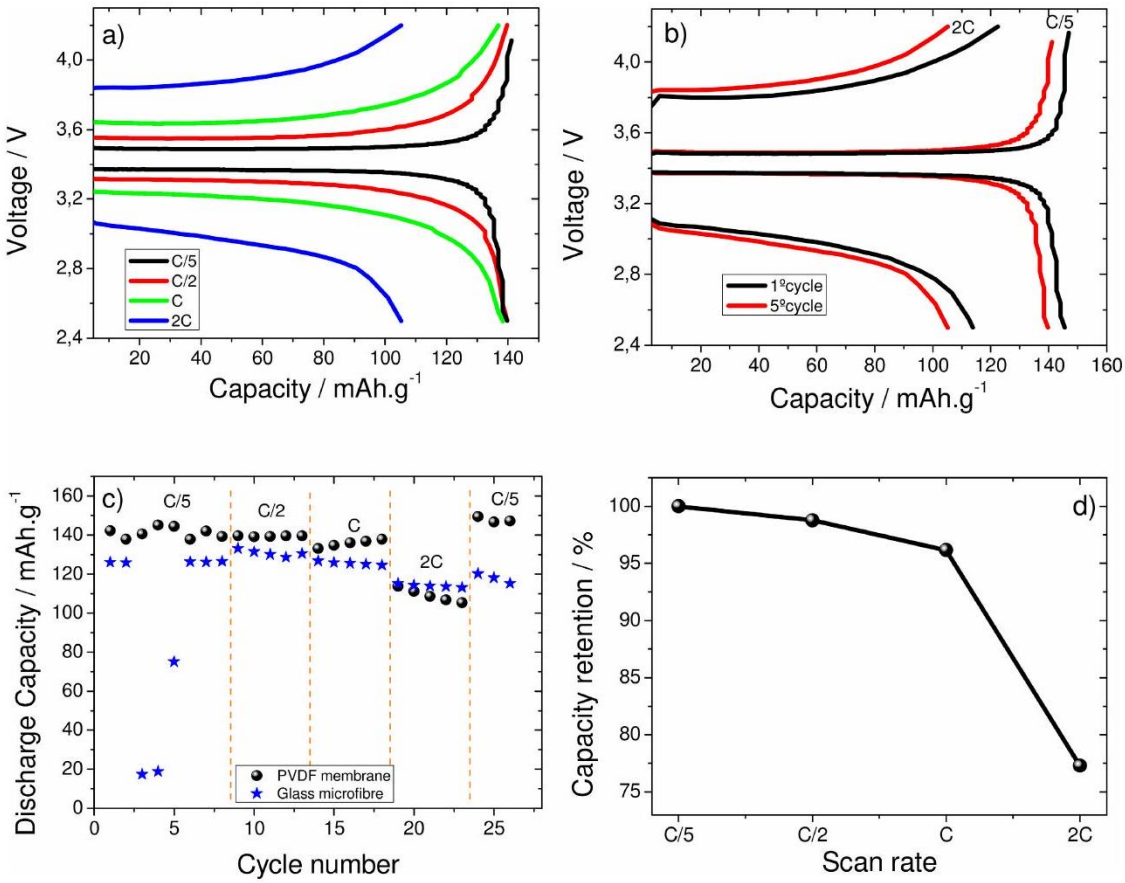

Figure 4. a) Charge-discharge profiles at different C-rates, (b) charge and discharge profiles at C/5 and 2C rate as a function of cycle number, (c) rate performances and (d) capacity retention in the discharge behavior for the PVDF membrane developed in this work. The rate performance of this sample was compared with a glass microfiber sample. redox reaction and is observed in Figures 4a)-c) independently of the **C**-rates and cycle number.

For $Li/C-LiFePOO_4$ cathodic half-cells using PVDF separator membranes, the discharge capacity value is $140mAh.g^{-1}$, $140mAh.g^{-1}$, $138mAh.g^{-1}$ and $105mAh.g^{-1}$ at rates of C/5, C/ 2, C and 2 C , respectively, which corresponds to 82%, 82%, 81% and 62% of the theoretical capacity of $C-LiFePO_4$ ($170mAh.g^{-1}$), indicating an excellent electrochemical stability even at higher rates.

It is also detected (Figure 4a) that the charge-discharge profiles decrease progressively as the C-rates increase, which is a result of the influence of ionic transport on ohmic polarization. [34]

The high rate capability up to C-rate can be ascribed to the better interfacial contacts between the electrolyte and the electrodes in the lithium-ion polymer cells with the PVDF membrane, which is ascribed to the fact that the PVDF polymer is the same for the separator and the cathode electrodes.

Figure 4b) shows the charge-discharge curves at the rates of C/5 and 2C for the PVDF separator membrane for 5 cycles. The discharge capacity for each C-rate shows that there

is no reactions associated to the electrochemical decomposition of the electrolyte as a function of time.

Figure 4c shows the rate capability in the discharge process of the PVDF membrane in comparison with a commercial glass microfibre separator, presenting a summary of the rate performance of 5 cycles for each rate ($C/5$ to $2C$) of the PVDF membranes and the glass microfibre separator.

Figure 4c) shows excellent cycling stability for $\mathrm{Li/C-LiFePO_4}$ cathodic half-cells using PVDF separator membranes, in particular at C-rates up to C, being higher than for the glass microfibre separator.

At C-rate, the PVDF membrane has a discharge capacity of $138\mathrm{mAh.g^{-1}}$ versus $124\mathrm{mAh.g^{-1}}$ for the glass microfibre separator. The excellent electrochemical performance of the PVDF membrane is due to the high electrochemical and interfacial stability.

Figure 4d) shows the capacity retention in the discharge process calculated by the normalization of the delivered capacity for each C-rate with respect to the nominal value for C/5 rate, as a function of C-rate for the PVDF membrane.

It is observed a small variation of the capacity retention up to C-rate, the capacity retention decreasing above this rate due to diffusion phenomena within the polymer electrolyte separator membrane (Figure 4d).

However, even for 2C (charge and/or discharge process in half an hour), the capacity retention of the PVDF membrane is 77% what is higher in comparison to the values observed for membranes prepared with the PVDF-HFP copolymer [14] for high degree of porosity value.

The cycling performance and the coulombic efficiency measured at C-rate for more than 50 cycles for the PVDF membrane are depicted in Figure 5a).

Cathodic half-cells prepared with the PVDF separator membranes show good cycling stability once the discharge capacity value after 50 cycles is $56\mathrm{mAh.^{-1}}$, corresponding to 50% of the capacity retention.

Moreover, the reason for the wave-like fluctuations of the discharge capacity values observed in Figure 5a) are not related to variations in the PVDF separator membrane, but to daily

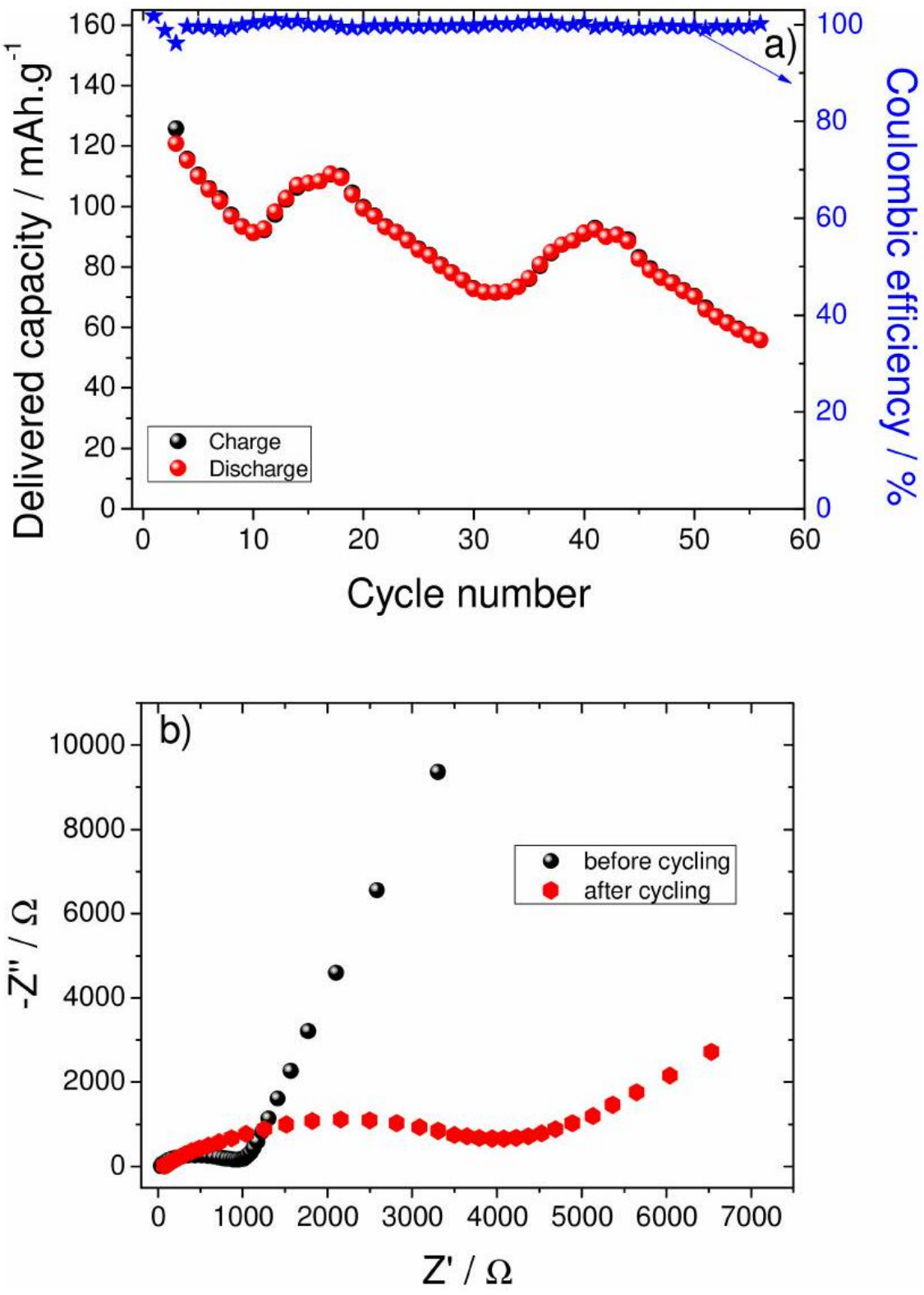

Figure 5. a) Discharge capacity and coulombic efficiency when cycled at Crate for the prepared PVDF membrane and (b) impedance spectroscopy of the cathodic half-cell before and after cycling.

fluctuation between day and night room temperature of the laboratory (~ 10°C), leading to variation of the battery temperature.

Figure 5a) also shows that the coulombic efficiency (CE), related to the reversibility of the process, is practically 100% over all the charge-discharge cycles.

In order to reach a more comprehensive understanding of the cycle performance of the cathodic half-cells assembled with the PVDF membrane, the ac impedance spectra of the half-cells were obtained before with in OCV (~ 3,2 V) and after cycling at ~ 2.9 V (Figure 5b), i.e, after rate performance (Figure 4c) and cycling performance (Figure 5a). Nyquist spectra for both curves indicated a semicircle (overall resistance) in the high and medium frequency regions and a straight line in the low frequency regions.

The overall resistance of the semicircle is the sum of the ohmic resistance (due to the liquid electrolyte), resistance that represents the contact film resistance (Li-ion migration resistance through the solid electrolyte interface (SEI) film formed on the cathode surface) and resistance contributions from the charge-transfer reaction resistance ascribed to the lithiumintercalation process. [35]

The overall resistance shown in Figure 5b) before and after cycling is 980Ω and 4070Ω, this increase being attributed due to the formation of SEI layer.

Moreover, the overall resistance value of the PVDF membrane after cycling indicates that the PVDF membrane form a stable SEI layer and facilitates the transport of Li^+ions through the interfacial film.

Electrochemical properties and battery performance of the PVDF membrane with ionic liquid

Based on the previous results on battery performance for the PVDF membrane, and to prove the concept of the possibility of a more environmentally friendly lithium-ion battery was fabricated by replacing the conventional electrolyte by a suitable ionic liquid for lithium-ion batteries. The ionic liquid used in this work was $[C_2mim][NTf_2]$ due to the high ionic conductivity (11mS/cm at room temperature) and low viscosity values (35 mPa at room temperature). [24] Further, this ionic liquid is very used due to its low volatility, low combustibility, high thermal stability and immiscibility in water. [36]

Figure 6a) shows the ionic conductivity value of the PVDF membrane soaked with ionic liquid as a function of temperature. It is shown that the ionic conductivity increases with increasing of the temperature from the room temperature value of $0.23 mS.cm^{-1}$ following an Arrhenius behavior.

The evaluation of the electrochemical window of the PVDF membrane soaked with ionic liquid was carried out by cyclic voltammetry (Figure 6b), showing a small current flow between 1.0 to 5.0 V (vs. Li^-/Li^+) which presents a stable window for lithium-ion battery applications.

The cycling performance of the PVDF membrane soaked with ionic liquid is illustrated in Figure 6c) as a function of the cycle number at C/5 rate. Initially, the discharge capacity value is 74.6mAh. g^{-1} and after 10 cycles, the value is 45mAh. g^{-1} representing a discharge capacity retention of 60%. The variation of the discharge capacity value as a function of the cycle number is due to the formation of SEI layer, which results in low compatibility towards Li metal and protection of lithium from corrosion. This fact is analyzed in detail in Figure 6d), which shows the Nyquist plots of the EIS measurements for cathodic half-cells incorporating the PVDF membrane before with in OCV (~ 3,2 V) and after cycling at ~ 2.9 V. Both curves exhibit two semicircles in the high-frequency range that represent the total resistance (sum of solid electrolyte interface (SEI) resistance and the charge-transfer resistances process) and an inclined line corresponds to the lithium-ion diffusion process, Warburg diffusion, at low frequencies. The total resistance shown in Figure 6d before and after cycling are 2100Ω and 38000Ω, the SEI resistance increasing with increasing cycle number and leading to reduced Li-ion diffusion and a significant increase of the interfacial resistance.

Discussion

It is the first time that this PVDF separator type is produced by green solvent, therefore Table 1 compares the physicochemical

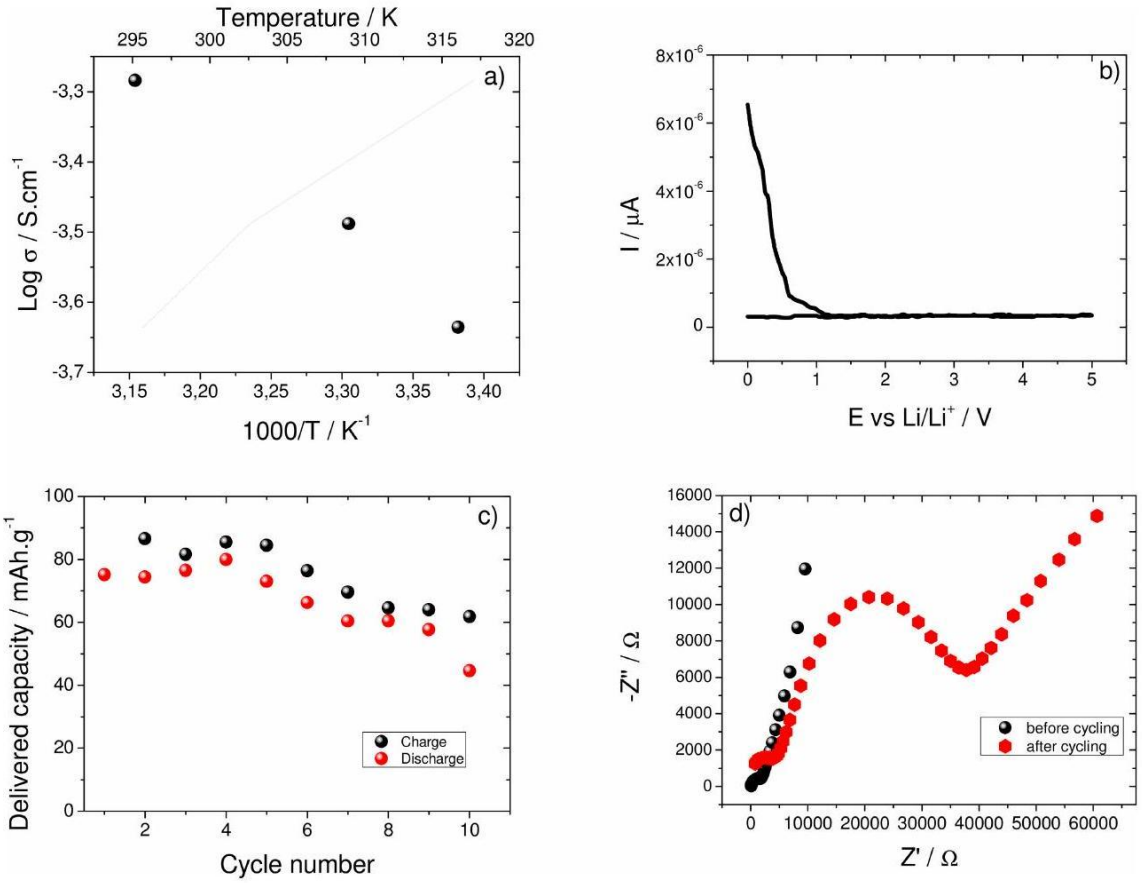

Figure 6. a) Ionic conductivity as a function of temperature, (b) electrochemical stability, (c) cycling performance at C/5-rate and (d) ac impedance before and after cycling for the PVDF membrane developed in this work soaked with ionic liquid.

Table 1. Ionic conductivity value, degree of porosity and discharge capacity for the PVDF membrane produced in this work in comparison with other PVDF separator membranes and green polymers reported in the literature. The electrolyte solution is indicated and the discharge capacity was determined with $CLiFePO_4$ cathode electrode.

Samples	oi / mS.cm-1	Porosity / %	Electrolyte solution	Capacity / mAh.g-1 at RT	Ref
PVDF	0.1	20	1 M LiPF6 in EC/DEC (1:1, v/v)	136 (C)	This work
PVDF/PEO - LAGP	7.7	83	1 M LiTFSI in EC:DEC (1:1 w/w).	150 (0.1C)	[37]
PVDF	0.30	-	1 M LiPF6 in EC/DMC/EMC	120 (0.2C)	[38]
PVDF-LiPAAOB electrospun composite	0.35	-	1 M LiPF6 in EC/DMC/EMC (1/1/1, w/w/w)	118 (0.2C)	[31]
PVDF/PPC membrane	4.05	85	1 M LiPF6 in EC/DMC (1:1, v/v)	160 (0.1C)	[39]
PVDF nanofiber	-	48	1 M LiPF6 in EC/DEC (4/6 ratio)	-	[40]
PVDF/PMMA membranes	1.21	-	1 M LiPF6 in EC:DMC (1:1 by volume	133 (0.2C)	[41]
Lignin	3.73	-	1 M LiPF6 in EC/DMC/ EMC (1/1/1, w/w/w)	137 (C)	[22]
Aramide membrane	1.1	70	1 M LiPF6 in EC:DEC (1:1 vol%)	~130 (0.5C)	[42]
Cellulose membrane	0.2	-	1 M LiPF6 in EC/DMC/EMC	130 (0.2C)	[21c]
Methyl celulose membrane	0.29	-	1 M LiPF6 in EC/DMC/EMC (1/1/1, w/w/w)	140 (0.2C)	[21b]

Cellulose fibers	0.014	-	1 M LiPF6 in EC:DEC (1:1 vol%)	100 (0.1C)	[21a]

and electrochemical properties of this separator membrane developed in this work with other PVDF membranes and green polymers reported in the literature for same electrode.

In some works, the degree of porosity value is not presented, but it can be stated that the value of the present sample is low when compared with the literature where its value is above of 50% in which the degree of porosity affect its ionic conductivity value.

Further, the ionic conductivity value of the prepared PVDF membrane is similar or lower in comparison to the values reported in the literature (Table 1).

Once the different electrolyte solutions presented in Table 1 show a similar conductivity value, the differences observed in the ionic conductivity values for the different samples are related to the microstructure, degree of porosity and electrolyte uptake value of the separator.

The discharge capacity value shown in Table 1 (the Figures related to battery performance for the PVDF membrane presented in the topic 3.3) in which for the PVDF membrane produced in this work are similar or in certain cases higher in comparison to other PVDF membranes and green polymers applied as battery separators depending of the C-rate. It is to notice that the electrochemical performance of this PVDF membrane is similar to the one obtained for PVDF membranes produced with N,N-dimethylformamide (DMF) (see supporting information, Figure S1).

Moreover, this work demonstrates that PVDF membrane is compatible with ionic liquid that is the next generation of the separator for lithium-ion battery with environmental friendly characteristics.

Conclusions

New separator membranes based on poly(vinylidene fluoride) (PVDF) have been prepared by solvent casting with N,N' dimethylpropyleneurea (DMPU).

A porous microstructure is obtained at $50°C$ with a degree of porosity about 20% and a pore size below 1μ m. The mechanical properties of the sample are suitable for lithium-ion batteries and its ionic conductivity, tortuosity and MacMullin number values are $0.1 mS.cm^{-1}, 4$ and 82, respectively.

The $Li/C - LiFePO_4$ half-cell battery based on this sample soaked in $1MLiPF_6$ in EC:DEC electrolyte solution shows good capacity and cycling properties up to high C-rates during 50 cycles. For this electrolyte solution, the discharge capacity value is $140mAh.g^{-1}, 140mAh.g^{-1}, 138mAh.g^{-1}$ and $105mAh.g^{-1}$ at rates of C/5, C/2, C and 2C, respectively

The half-cells fabricated based on this sample with ionic liquid represents a step toward a more environmental friendly lithium-ion battery that shows a discharge capacity value of $45mAh.g^{-1}$ at C/5-rate and discharge capacity retention of 60%, after 10 cycles.

Taking into account the electrochemical performance for both systems (electrolyte solution and ionic liquid), this new separator is an appropriate candidate for their use in safer lithium-ion batteries applications and represent an advance in new battery separator types produced by a "green solvent" and green electrolyte approach.

Acknowledgements

This work was supported by the Portuguese Foundation for Science and Technology (FCT) in the framework of the Strategic Funding UID/FIS/04650/2013. The authors thank FEDER funds through the COMPETE 2020 Programme and National Funds through FCT under the projects PTDC/CTM-ENE/5387/2014 and UID/CTM/50025/2013 and grants SFRH/BD/90313/2012 (A.G.), and SFRH/BPD/112547/2015 (C.M.C.). The authors acknowledge funding by the Spanish Ministry of Economy and Competitiveness (MINECO) through the project MAT2016-76039-C4-3-R (AEI/FEDER, UE) and from the Basque Government Industry Department under the ELKARTEK program. The authors thank Solvay, Timcal and Phostech for kindly supplying the high quality materials.

Keywords: Green solvent • lonic liquid • Lithium-ion batteries • PVDF separator

1] a) R. Huggins, Advanced Batteries: Materials Science Aspects, Springer US, 2008; b) V. Etacheri, R. Marom, R. Elazari, G. Salitra, D. Aurbach, Energy Environ. Sci. 2011, 4, 3243-3262; c) P. G. Bruce, B. Scrosati, J.-M. Tarascon, Angew. Chem., Int. Ed. 2008, 47, 2930-2946.
[2] a) N. Nitta, F. Wu, J. T. Lee, G. Yushin, Mater. Today 2015, 18, 252-264; b) J. W. Choi, D. Aurbach, Nat. Rev. Mater. 2016, 1, 16013.
[3] J. Twidell, T. Weir, Renewable Energy Resources, Taylor & Francis, 2015.
[4] a) J. M. Tarascon, M. Armand, Nature 2001, 414, 359-367; b) B. Scrosati, J. Garche, J. Power Sources 2010, 195, 2419-2430; c) K. Amine, R. Kanno, Y. Tzeng, MRS Bull. 2014, 39, 395-401.
[5] a) C. M. Costa, M. M. Silva, S. Lanceros-Mendez, RSC Adv. 2013, 3, 1140411417; b) J. Nunes-Pereira, C. M. Costa, S. Lanceros-Méndez, J. Power Sources 2015, 281, 378-398.
[6] L. Long, S. Wang, M. Xiao, Y. Meng, J. Mater. Chem. A 2016, 4, 1003810069.
[7] X. Gao, W. Sheng, Y. Wang, Y. Lin, Y. Luo, B.-G. Li, J. Appl. Polym. Sci. 2015, 132, n/a-n/a.
[8] H. Liu, J. Xu, B. Guo, X. He, J. Mater. Sci. 2014, 49, 6961-6966.
[9] C. M. Costa, J. Nunes-Pereira, L. C. Rodrigues, M. M. Silva, J. L. G. Ribelles, S. Lanceros-Méndez, Electrochim. Acta 2013, 88, 473-476.
[10] A. Subramania, N. T. K. Sundaram, G. V. Kumar, J. Power Sources 2006, 153, 177-182.
[11] C. S. Kim, S. M. Oh, J. Power Sources 2002, 109, 98-104.
[12] N. Muniyandi, N. Kalaiselvi, P. Periyasamy, R. Thirunakaran, B. Ramesh Babu, S. Gopukumar, T. Premkumar, N. G. Renganathan, M. Raghavan, J. Power Sources 2001, 96, 14-19.
[13] C. M. Costa, J. L. Gomez Ribelles, S. Lanceros-Méndez, G. B. Appetecchi, B. Scrosati, J. Power Sources 2014, 245, 779-786.
[14] R. E. Sousa, J. Nunes-Pereira, C. M. Costa, M. M. Silva, S. LancerosMéndez, J. Hassoun, B. Scrosati, G. B. Appetecchi, J. Power Sources 2014, 263, 29-36.
[15] R. E. Sousa, M. Kundu, A. Goren, M. M. Silva, L. Liu, C. M. Costa, S. Lanceros-Mendez,

RSC Adv. 2015, 5, 90428-90436.
[16] P. Martins, A. C. Lopes, S. Lanceros-Mendez, Prog. Polym. Sci. 2014, 39, 683-706.
[17] K. Romanyuk, C. M. Costa, S. Y. Luchkin, A. L. Kholkin, S. LancerosMéndez, Langmuir 2016, 32, 5267-5276.
[18] a) M.-M. Tao, F. Liu, B.-R. Ma, L.-x. Xue, Desalination 2013, 316, 137-145; b) M. Li, I. Katsouras, C. Piliego, G. Glasser, I. Lieberwirth, P. W. M. Blom, D. M. de Leeuw, J. Mater. Chem. C 2013, 1, 7695-7702.
[19] J. M. Stellman, Encyclopaedia of Occupational Health and Safety, International Labour Office, 1998.
[20] C. Capello, U. Fischer, K. Hungerbuhler, Green Chem. 2007, 9, 927-934.
[21] a) L. Jabbour, M. Destro, D. Chaussy, C. Gerbaldi, N. Penazzi, S. Bodoardo, D. Beneventi, Cellulose 2013, 20, 571-582; b) M. Li, X. Wang, Y. Wang, B. Chen, Y. Wu, R. Holze, RSC Adv. 2015, 5, 52382-52387; c) S. Xiao, F. Wang, Y. Yang, Z. Chang, Y. Wu, RSC Adv. 2014, 4, 76-81.
[22] S.-D. Gong, Y. Huang, H.-J. Cao, Y.-H. Lin, Y. Li, S.-H. Tang, M.-S. Wang, X. Li, J. Power Sources 2016, 307, 624-633.
[23] a) D. Prat, A. Wells, J. Hayler, H. Sneddon, C. R. McElroy, S. Abou-Shehada, P. J. Dunn, Green Chem. 2016, 18, 288-296; b) A. Mouret, L. Leclercq, A. Muhlbauer, V. Nardello-Rataj, Green Chem. 2014, 16, 269-278.
[24] L. Sun, O. Morales-Collazo, H. Xia, J. F. Brennecke, J. Phys. Chem. B 2015, 119, 15030-15039.
[25] J. C. C. Ferreira, T. S. Monteiro, A. C. Lopes, C. M. Costa, M. M. Silva, A. V. Machado, S. Lanceros-Mendez, J. Non-Cryst. Solids 2015, 412, 16-23.
[26] P. Kneisl, J. W. Zondlo, J. Chem. Eng. Data 1987, 32, 11-13.
[27] C. J. Orendorff, Electrochem. Soc. Interface 2012, 21, 61-65.
[28] H. Lee, M. Yanilmaz, O. Toprakci, K. Fu, X. Zhang, Energy Environ. Sci. 2014, 7, 3857-3886.
[29] G. Y. Gor, J. Cannarella, C. Z. Leng, A. Vishnyakov, C. B. Arnold, J. Power Sources 2015, 294, 167-172.
[30] B.-Y. Chang, S.-M. Park, Annu. Rev. Anal. Chem. 2010, 3, 207-229.
[31] Y. Zhu, S. Xiao, Y. Shi, Y. Yang, Y. Wu, J. Mater. Chem. A 2013, 1, 77907797.
[32] J. Landesfeind, J. Hattendorff, A. Ehrl, W. A. Wall, H. A. Gasteiger, J. Electrochem. Soc. 2016, 163, A1373-A1387.
[33] A. Gören, C. M. Costa, M. M. Silva, S. Lanceros-Méndez, Composites, Part B 2015, 83, 333-345.
[34] W. Xiao, L. Zhao, Y. Gong, S. Wang, J. Liu, C. Yan, RSC Adv. 2015, 5, 34184-34190.
[35] A. Gören, J. Mendes, H. M. Rodrigues, R. E. Sousa, J. Oliveira, L. Hilliou, C. M. Costa, M. M. Silva, S. Lanceros-Méndez, J. Power Sources 2016, 334, 65-77.
[36] T. R. Jow, K. Xu, O. Borodin, U. Makoto, Electrolytes for lithium and lithium-ion batteries, Vol. 58, Springer, 2014.
[37] N. Shubha, R. Prasanth, H. H. Hng, M. Srinivasan, J. Power Sources 2014, 267, 48-57.
[38] Y. Zhu, F. Wang, L. Liu, S. Xiao, Z. Chang, Y. Wu, Energy Environ. Sci. 2013, 6, 618-624.
[39] X. Huang, S. Zeng, J. Liu, T. He, L. Sun, D. Xu, X. Yu, Y. Luo, W. Zhou, J. Wu, J. Phys. Chem. C 2015, 119, 27882-27891.
[40] K. Hwang, B. Kwon, H. Byun, J. Membr. Sci. 2011, 378, 111-116.
[41] N. H. Idris, M. M. Rahman, J.-Z. Wang, H.-K. Liu, J. Power Sources 2012, 201, 294-300.
[42] J. Zhang, Q. Kong, Z. Liu, S. Pang, L. Yue, J. Yao, X. Wang, G. Cui, Solid State Ionics 2013, 245-246, 49-55.